THE JOURNAL OF PHYSICAL CHEMISTRY B

Article

pubs.acs.org/JPCB

Measurement of the Hydrodynamic Radius of Quantum Dots by Fluorescence Correlation Spectroscopy Excluding Blinking

A. A. de Thomaz,[†] D. B. Almeida,[†] V. B. Pelegati,[†] H. F. Carvalho,[‡,§] and C. L. Cesar*[,†,§]

[†]Department of Quantum Electronics, Institute of Physics "Gleb Wataghin", State University of Campinas/UNICAMP, 13083-859 Campinas, São Paulo, Brazil

[‡]Department of Structural and Functional Biology, Institute of Biology, State University of Campinas/UNICAMP, 13083-865 Campinas, São Paulo, Brazil

[§]National Institute of Photonics Applied to Cell Biology (INFABIC), 13083-865 Campinas, São Paulo, Brazil

ABSTRACT: One of the most important properties of quantum dots (QDs) is their size. Their size will determine optical properties and in a colloidal medium their range of interaction. The most common techniques used to measure QD size are transmission electron microscopy (TEM) and X-ray diffraction. However, these techniques demand the sample to be dried and under a vacuum. This way any hydrodynamic information is excluded and the preparation process may alter even the size of the QDs. Fluorescence correlation spectroscopy (FCS) is an optical technique with single molecule sensitivity capable of extracting the hydrodynamic radius (HR) of the QDs. The main drawback of FCS is the blinking phenomenon that alters the correlation function implicating in a QD apparent size smaller than it really is. In this work, we developed a method to exclude blinking of the FCS and measured the HR of colloidal QDs. We compared our results with TEM images, and the HR obtained by FCS is higher than the radius measured by TEM. We attribute this difference to the cap layer of the QD that cannot be seen in the TEM images.

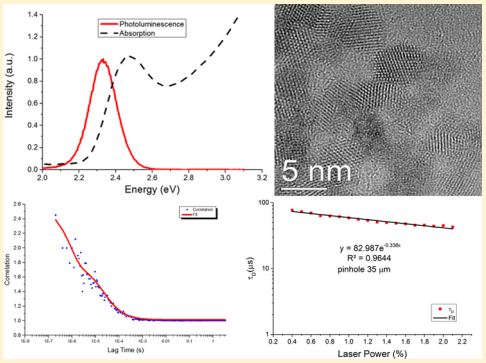

INTRODUCTION

The main reason quantum dots (QDs) attracted great attention of the scientific community was the possibility to tailor their optical properties controlling the size, which opens up a great deal of applications. Size and the relation between sizes and the optical properties (associated with confinement effects) are, therefore, the most important parameters for any QD application. This shows the importance to measure the QD size together with its optical properties for the design of any QD based device. QD applications are based on the following optical properties: light emission (displays,[1] lasers,[2] fluorescent markers for biology); light absorption (photovoltaics,[3,4] photodetectors[5]); and nonlinear optical properties (optical switches[6]). For all light emission devices, it is mandatory to avoid as much as possible the presence of surface traps that decreases the emission efficiency. The way to do that is to create a larger band gap cap layer to export these traps to the outer surface and to shield the inner core QD to avoid energy/charge transfer or confinement changes. Hence, the cap layer size must be taken into account in the measurement of the QD size. In the area of fluorescent markers, colloidal QDs (CQDs) have become an important alternative to the commonly used organic dyes.[7] CQDs have been reported to be 20 times brighter and 100 times more stable than conventional fluorescent dyes.[8] The conjugation of the cap layer with special molecules can provide high specificity to these QD markers. Finally, QD cytotoxicity is almost nonexistent.[9] For biological applications, QDs must be immersed in aqueous solution to interact with cells, which means that the ideal measurements of QD properties must be performed in the liquid solution, especially the QD size, since the QD hydrodynamic radius (HR) determines its range of interaction. Moreover, any modification in the surface of the cap layer should also be measured in the colloidal form.

However, the commonly used techniques to measure the QD size demand them to be in a dry and isolated environment, like transmission electronic microscopy (TEM) or X-ray diffraction (XRD). Despite the information with high precision of these techniques, the fact that the QDs are not in their colloidal form does not provide the HR values and hides its interaction with the environment. Besides the fact that the whole process of sample preparation is tedious and time-consuming, it can cause artifacts like agglomerations or QD extra growth during the drying process. In the TEM case, the sizes of the QDs are measured by the analysis of hundreds of visible particles in the acquired images, representing a poor statistics in the determinations of the average size. The XRD technique, on the other hand, is capable of analyzing a great number of particles. Nevertheless, this measurement provides average values over the whole ensemble, missing the single particle

Received: December 8, 2014
Revised: February 5, 2015
Published: February 18, 2015

ACS Publications © 2015 American Chemical Society

DOI: 10.1021/jp512214p
J. Phys. Chem. B 2015, 119, 4294−4299

sensitivity. There is a more fundamental question for these measurements: TEM/XRD only "sees" the nuclei of the atoms, not the electronic cloud. However, it is the size of the potential that confines the electron, which spreads beyond the last nucleus of the QD, which defines the optical properties.

In this scenario, fluorescence correlation spectroscopy (FCS) developed by Madge, Elson, and Webb[10] is a technique that offers the possibility of single molecule detection, averaging over a huge number of particles in the colloidal environment. Although the technique was developed before the first commercial laser scanning confocal microscopy, Bio-Rad MRC 500[11] in 1989, the number of publications jumped after the adaption of the FCS in the confocal microscopes.[12,13] Since then, it has been used to noninvasively monitor the diffusion and dynamics of DNA−drug interactions. FCS requires almost no sample preparation and is nondestructive, in contrast with TEM and XRD, which require the sample to be in a vacuum and dried. FCS will take into account even the cap layer, since the HR is intrinsically extracted from the correlation curve. On the basis of these facts, we believe that FCS is one of the most suitable techniques to measure the QD size in aqueous solution.

The fact that FCS presents single molecule detection makes it sensitive to the phenomenon of QD blinking,[14] which can affect the measurements. Blinking, the intermittency in the fluorescence of a particle, is only observed in single molecule experiments, since the average over the ensemble masks this effect. The fluorescence intermittency alters the correlation curve, resulting in an apparent diffusion time different from the real diffusion time without blinking. Usually, the literature excludes this effect in the analysis by the following argument: blinking is negligible[15−17] for low intensities of the excitation laser. However, we found that this argument is not reproducible and not reliable. In our measurements, even the lowest excitation power generates a FCS curve with blinking features. Therefore, we present in this paper a method to use the FCS technique to measure the HR of CdTe CQDs in the presence of blinking.

FLUORESCENCE CORRELATION SPECTROSCOPY

In "modern" FCS, a photocounter detects the photons emitted by molecules diffusing inside the focal volume. A correlation curve as a function of time is obtained by the fluctuations of the fluorescence intensity due to Brownian motion. The FCS autocorrelation function (ACF) is given by[10,18,19]

$$G(\tau) = \frac{\langle \delta F(t)\delta F(t+\tau)\rangle}{\langle F(t)\rangle^2} \tag{1}$$

where $\delta F(t)$ is the fluorescence fluctuation, $F(t)$ is the fluorescence signal, and τ is the time delay. Assuming a 3D diffusion and a Gaussian laser beam, eq 1 takes the form

$$G(\tau) = \frac{1}{\langle N\rangle}\frac{1}{\left(1+\frac{\tau}{\tau_D}\right)}\frac{1}{\sqrt{\left(1+\left(\frac{\omega_x}{\omega_z}\right)^2\frac{\tau}{\tau_D}\right)}} \tag{2}$$

The three parameters that can be extracted from the fitting of the ACF are the average number of fluorescent particles in the focal volume ($\langle N\rangle$), the characteristic diffusion time of the particle (τ_D), and the ratio between the lateral/axial radii ω_x/ω_z. These radii are defined as the distance at which the intensity of the laser beam is decreased to e^{-2}. Although the Gaussian beam assumption is not a good approximation for the focal region of a high numerical aperture beam, it provides a very satisfactory[20] description after the use of the pinhole to diminish the focal volume. The particle concentration must be small because of the $\langle N\rangle^{-1}$ dependence of the ACF but still high enough to generate a detectable signal. Typically, one uses $\langle N\rangle = 1$ to $\langle N\rangle = 10$ molecules in the focal volume, which translates into nanomolar concentrations for a focal volume of the order of femtoliters.[12] The diffusion time τ_D is related to the diffusion coefficient D by

$$\tau_D = \frac{\omega_x^{\,2}}{4D} \tag{3}$$

For spherical particles, the diffusion coefficient is connected to the particle radius (R) through the Stokes−Einstein equation

$$R = \frac{kT}{6\pi\eta D} \tag{4}$$

where k is the Boltzmann constant, η is the medium viscosity, and T is the temperature. Particle diameters are obtained from the diffusion time τ_D knowing the size of the lateral radius ω_x of the laser beam. This lateral radius can be calculated from the FCS curve of a molecule with a known diffusion coefficient. In the autocorrelation curve of eq 2, only the Brownian motion is responsible for the fluctuation in the fluorescence signal. The ACF can be easily modified to eq 5 in the presence of another fluorescence fluctuation not related to the Brownian motion when the characteristic time scale is much shorter, or longer, than the diffusion.

$$G(\tau) = G(\tau)_{\text{diffusion}}\cdot G(\tau)_{\text{phenomenon}} \tag{5}$$

The singlet−triplet simple exponential decay transitions are the classical example of this where the ACF is given by[21]

$$G(\tau) = \left(1+\frac{T e^{-\tau/\tau_{\text{triplet}}}}{1-T}\right)\frac{1}{\langle N\rangle}\frac{1}{\left(1+\frac{\tau}{\tau_D}\right)} \times \frac{1}{\sqrt{\left(1+\left(\frac{\omega_x}{\omega_z}\right)^2\frac{\tau}{\tau_D}\right)}} \tag{6}$$

where T is the fraction of particles in the triplet state with a lifetime of τ_{triplet}.

The Apparent Effect of Blinking in the Diffusion Time.

Fluorophores, especially QDs, can blink. Blinking is characterized by a time interval in an "off" state, where no emission occurs, and another period in the "on" state, where fluorescence is present. It is known that the probability distribution of the "off" times follows a power law distribution[14]

$$P(t) = At^{-\alpha} \tag{7}$$

with the α coefficient assuming values between 1.4 and 1.7.[14] The "on" times also follow a power law, with the same coefficient, although it presents a saturation effect dependent on the temperature and laser power.[14] This fact means that the time interval a QD emits before going into an "off" state is affected by laser power and, consequently, the FCS measurement. Blinking has been observed in a time scale from 200 μs to 10 s,[15] in the range of the time scale of the ACF that spans from zero to 1 ms; therefore, it cannot be simply incorporated by the product of two independent ACFs as in eq 6. The time scale of

DOI: 10.1021/jp512214p
J. Phys. Chem. B 2015, 119, 4294−4299

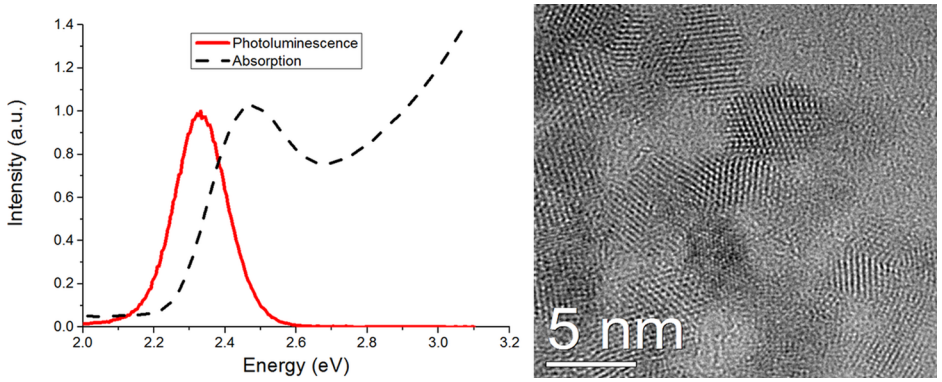

Figure 1. Absorbance (dashed curve) and photoluminescence (solid curve) spectra and a transmission electron microscopy image.

diffusion in our QDs is in the order of 100 μs, meaning that QD fluorescence can disappear for a time, i.e., blinks, before it leaves the excitation volume. The apparent effect of blinking for the ACF is like if the molecule left the focal volume much faster than diffusion, resulting in a diffusion time shorter than the real one. Moreover, because the blinking ratio increases with the excitation power, one expects apparent power dependent diffusion times, which has been observed before.[15,16]

EXPERIMENTAL SETUP

CdTe Quantum Dot Preparation. We prepared CdTe QDs using an aqueous method and thiol capping, based on the synthesis of Zhang et al.[22,23] In a sealed flask, under an argon atmosphere and magnetic agitation, 40 mL of water and 38 mg of tellurium powder (Aldrich; 99.997%; >40 mesh) were heated up to 80 °C. In parallel, 66.8 mg of $NaBH_4$ (Aldrich; >96%) was dissolved in 5 ml of water and then added to the previous 80 °C solution to reduce the Te into Te^{-2}. The reduction process was kept under the same conditions for 2 h. To prepare the cadmium and thiol mixed solution, we added 0.52 mL of a 0.1 mol/L solution of cadmiun perchlorate (Aldrich; >99.9%) into 0.24 mL of 5% mercaptoacetic acid (MAA; Sigma-Aldrich; >99%) solution under atmospheric conditions. The pH of the final solution was adjusted to 11.2 with a highly concentrated NaOH water solution.

This solution was quickly added to the reduced tellurium by injection through a rubber septum, after which the temperature was increased to 100 °C and kept under stirring for a given time. This last heating step controls the QD size growth and accelerates the proper QD thiol surface coating to enhance its emission efficiency. Because QDs become bigger with time, we can select its emission color from blue to red by this treatment time, which ends with a sample cooling down and storage in a refrigerator. The 30 min treatment time produced green fluorescent QDs.

Size Measurement by Transmission Electron Microscopy. The measurement of the QD sizes and dispersion was made by TEM in the same sample used to perform FCS, without any other procedure. A droplet of the original colloid sample, as prepared, was dripped into a carbon film coated copper grid and put to rest for drying for several hours. The images were acquired in a 300 kV JEOL 3010 electron microscope and processed using ImageJ software. We measured 233 particles manually, one by one, considering all the particles as spheres and drawing circles around them, calibrated by the scale bar. From these measurements, we obtained an average radius and standard error of the mean of 1.58 ± 0.03 nm and standard deviation of 0.42 nm, correspondingly to a 28% size dispersion. Figure 1 shows the room temperature absorbance (dashed) and the photoluminescence (PL) (solid) spectra together with a transmission electron microscopy image of a set of quantum dots used in this work. We specifically chose these homemade QDs because we wanted a QD composed by the semiconductor core and a cap layer that we could know the size. This way we can compare the results of the TEM images with the FCS HR measurement and obtain information about the cap layer that is not provided by the TEM measurement.

FCS Microscopy. For FCS measurements, we filtered the sample with a 200 nm Millipore filter to eliminate eventual particle clusters that generate spikes of intense emissions and compromise the experiment. The measurements were performed in a Zeiss Spectral Confocal Microscope LSM 780 upright (Carl-Zeiss, Jena, Germany) with a Zeiss Plan-Apochromat 40×/1.0 Water DIC (WD: 2.5 mm) objective. This objective was covered with plastic to enable its immersion directly into the liquid solution. We also used an external objective heater (Bioptechs - Butler, USA) to keep the sample temperature constant at 30 °C. The fluorescence was excited with the 488 nm line of the argon laser and the descanned signal detected with an Avalanche Photodiode Array (APDs) after the pinhole.

We used the Zeiss control software (Zen 2010) in the FCS mode, where the laser beam is fixed at only one point at the optical axis of the system, and the photocounting mode of the APDs is enabled. This software also calculates the correlation curve and performs the fitting. We made an average of 20 curves obtained during 10 s each, discarding curves that presented spikes of fluorescence due to the presence of QD clusters. To keep all measurements in the same conditions, we always discarded 10 curves, even for the cases where only 3 curves presented the spikes.

RESULTS FOR HYDRODYNAMIC RADIUS MEASURED BY FCS

Calibration of the Lateral Radius. A calibration for each pinhole diameter was made using rhodamine B, a dye with a well-known ($D = (4.27 \pm 0.04) \times 10^{-6}$ cm^2 s^{-1} at 25 °C) water diffusion coefficient.[24] We corrected the diffusion coefficient value for the 30 °C temperature used in our experiment using the formula

$$D_{30^\circ C} = \frac{\eta_{25^\circ C}}{\eta_{30^\circ C}} \times \frac{T_{30^\circ C}}{T_{25^\circ C}} \times D_{25^\circ C} \quad (8)$$

DOI: 10.1021/jp512214p
J. Phys. Chem. B 2015, 119, 4294−4299

where T is the temperature in Kelvin, $D_{25°C} = (4.27 \pm 0.04) \times 10^{-6}$ cm^2 s^{-1}, $\eta_{25°C} = 890$ mPa·s and $\eta_{30°C} = 0.797$ mPa·s are the water viscosity,[25] to obtain the value $D_{30°C} = (4.85 \pm 0.04) \times 10^{-6}$ cm^2 s^{-1}.

The dye was diluted in Milli-Q water until a concentration in the order of nanomolar was reached, and 40 μL of the solution was dropped on top of a microscopy slide. Figure 2 shows a typical rhodamine ACF curve obtained with a fitting including the singlet−triplet transition. For each pinhole size, we measured the diffusion time of 10 FCS curves from which we obtained 10 values of ω_x using eq 3. The calibration was performed assigning the 10 curves ω_x average for the lateral radii of each pinhole, as shown in Table 1.

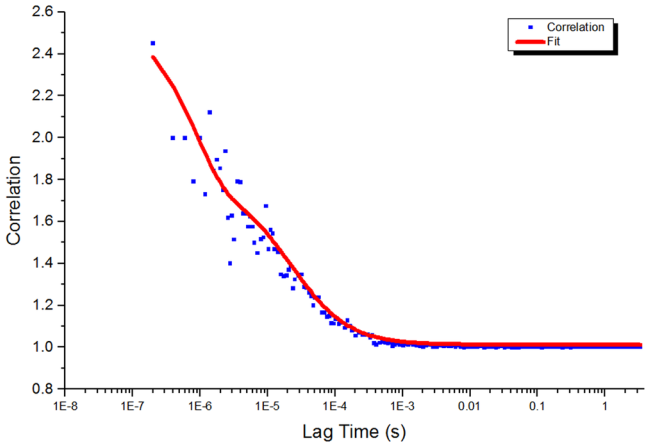

Figure 2. ACF for RB and fit.

Table 1. Calibration of ω_x for Each Pinhole Size Using the 488 nm Argon Laser Line

pinhole (μm)	τ_D (μs)	ω_x (μm)
20	20.1 ± 0.5	197 ± 3
25	22.4 ± 0.5	209 ± 3
30	23.5 ± 0.5	214 ± 3
35	23.8 ± 0.5	215 ± 3
40	25.7 ± 0.5	223 ± 3
45	26.9 ± 0.5	228 ± 3
50	28.9 ± 0.5	237 ± 3
55	29.0 ± 0.5	237 ± 3
60	30.4 ± 0.5	243 ± 3
65	31.3 ± 0.5	246 ± 3

Results of QD Hydrodynamic Radius with FCS. To measure the QD FCS curves, we repeated the procedure used with rhodamine B: 40 μL of the solution on top of a microscopy slide and measurement of 10 FCS curves for each laser power and pinhole size. The pinhole size varied from 20 to 65 μm in 5 μm steps, and we used the average over the 10 curves as the final result for the diffusion time for each excitation power and pinhole size.

Table 2 shows the values of the number of particles and diffusion time τ_D for different excitation powers for a pinhole size of 35 μm. We observed a continuous decay of the diffusion time as the power increases from the lowest excitation power capable of generating a detectable fluorescence signal. This fact indicates the occurrence of blinking even for these low excitation powers. This brings doubts about the usual procedure of the literature to use FCS to measure HR of QDs at low power, where the blinking would be negligible[15−17,26]

Table 2. Values of Apparent Diffusion Time and Number of Particles of the CdTe QDs for Different Laser Powers and a 35 μm Pinhole

laser power (%)	number of particles	app. diff. time (μs)
0.4	2.1	76.9 ± 0.5
0.5	2.0	73.0 ± 0.5
0.6	1.8	69.6 ± 0.5
0.7	1.7	63.3 ± 0.5
0.8	1.7	62.5 ± 0.5
0.9	1.7	61.2 ± 0.5
1.0	1.6	58.7 ± 0.5
1.1	2.9	55.9 ± 0.5
1.2	2.1	53.8 ± 0.5
1.3	2.1	50.8 ± 0.5
1.4	2.1	49.7 ± 0.5
1.5	2.2	48.8 ± 0.5
1.6	2.2	47.8 ± 0.5
1.7	2.3	45.4 ± 0.5
1.8	2.3	45.7 ± 0.5
1.9	2.4	44.0 ± 0.5
2.0	2.5	44.8 ± 0.5
2.1	2.5	42.8 ± 0.5

The correct diffusion time in the absence of blinking can only be measured in the limit of zero excitation power. To obtain this limit, we fitted the apparent diffusion time with $\tau_D = \tau_0 e^{P/P_0}$ shown in the semilog plot of Figure 3. In this case, τ_0 is the real diffusion time in the absence of blinking. As we can see from Figure 3, the extrapolation provided the value of $\tau_0 = 83$ μs, significantly higher than $\tau_0 = 77$ μs obtained at the lowest excitation power. We repeated this fitting procedure to measure τ_0 for all pinhole sizes (data not shown) and translated the results to QD HR in Table 3 using eq 4 and the ω_x obtained with the calibration procedure for each pinhole size. The laser power range selected for the measurement was the range proposed by the argument that blinking is negligible at low laser power. The average HR and the standard error of the mean of the CdTe QD was 1.95 ± 0.03 nm with a standard deviation of 0.09 nm, resulting in 5% dispersion.

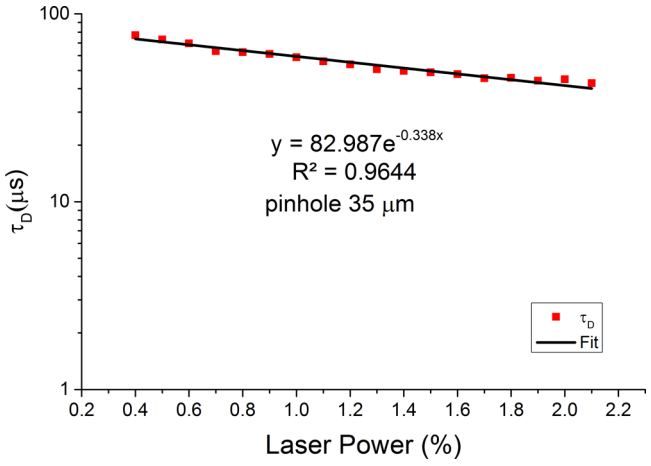

Figure 3. Graph of the diffusion time of CdTe QDs for 35 μm pinhole size.

DOI: 10.1021/jp512214p
J. Phys. Chem. B 2015, 119, 4294−4299

Table 3. QD HR as a Function of Pinhole Size

pinhole (μm)	HR (nm)
20	1.94 ± 0.01
25	1.87 ± 0.01
30	1.97 ± 0.01
35	2.01 ± 0.01
40	1.87 ± 0.01
45	2.13 ± 0.01
50	1.89 ± 0.01
55	1.95 ± 0.01
60	1.83 ± 0.01
65	2.03 ± 0.01
mean ± std. error	1.95 ± 0.03
std. dev.	0.09

We obtained an average HR radius of 1.95 ± 0.03 nm and a dispersion of 5% with the method presented in this paper, while the TEM measurements presented a value of 1.58 ± 0.03 nm with a dispersion of 28%. We atribute this difference to the nature of the techniques itself. The TEM measurement is done on a small part of the QD population; although the FCS measurement has single molecule sensitivity, the final result is an average over the ensemble. Only particles that have been dried and kept their circular/spherical form are counted in TEM. Moreover, in TEM, all particles that are visible in the micrograph have their sizes measured, independently if they are emitting fluorescence or not. Particles with defects in the crystalline structure, with incomplete passivation, and with any other defect would not emit fluorescence; however, their sizes are measured in the TEM images and hence increase the dispersion calculation. On the other hand, in FCS, only fluorescent particles are measured. The fluorescence emission energy of a single QD is directly related to its size, which means that the dispersion in the fluorescence emission spectra would be directly related to the QD size dispersion. We fitted a Gaussian function to the emission spectra of our QD in Figure 1 and obtained a mean energy emission and standard error of the mean of 2.33 ± 0.01 eV with a standard deviation of 0.08 eV. From the emission spectra measurement, we obtain a dispersion of 3.4% which is in a good agreement with the dispersion obtained with our method of 5%. The difference of the TEM radius and the FCS HR is 0.37 nm, which corresponds to 2.5 carbon−carbon 0.15 nm bonds, compatible with the mercaptoacetic acid, Figure 4, used as the cap layer of our QDs. The hydrogen of HS dissolves, and the sulfur atom binds directly to the Cd QD atoms.

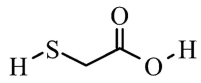

Figure 4. Molecule of mercaptoacetic acid.

CONCLUSION

In this paper, we presented a method to measure the QD HR using the FCS technique excluding blinking. The HR is extracted intrinsically from the correlation curve, and any modification to the cap layer is automatically taken into account in the FCS measurement as well. The measurements with FCS can be done almost in real time; aliquots of the original sample can be extracted while it undergoes any modification processes. This is impossible to do with TEM or XRD because the sample must be dried and in a vacuum. All of this processing for TEM and XRD may alter the properties and even the size of the QDs. With our method, we excluded blinking which was a problem for applying FCS to measure the HR of QD. The previous argument that blinking is negligible at low laser powers was too vague, and it could be difficult to reproduce with different equipment. The method presented in this paper is reproducible and can be applied in any system capable of performing FCS measurements with a variable power laser source. The QD HR measured by FCS was higher than the size measured by TEM. We attribute the difference between these values as being due to the cap layer of the QD that is not visible in the TEM images. The size dispersion measured by TEM is higher than the size dispersion measured by FCS. We believe this is reasonable because of several factors. First, the TEM measurements are a direct sampling of the parent population, while each FCS measurement is composed by an average of several particles. Our 5% dispersion was obtained from several FCS ACFs, each one an average itself. The average dispersion is always lower than the parent population dispersion. FCS can be better compared to fluorescence, which is also an average of several particles. Both FCS and fluorescence only see fluorescent particles, while TEM sees all of them, increasing the size dispersion measured. Because of the direct relation of QD size and fluorescence emission energy, we obtained a size dispersion from FCS that is in agreement with the emission energy dispersion measured in the fluorescence emission spectra. Taking into account all of these facts presented in this paper, we believe FCS is one of the most powerful techniques to extract information about QDs in a colloidal environment.

AUTHOR INFORMATION

Corresponding Author

*E-mail: lenz@ifi.unicamp.br.

Notes

The authors declare no competing financial interest.

ACKNOWLEDGMENTS

A.A.d.T. was a recipient of a fellowship of the State of São Paulo Funding Agency (FAPESP). FAPESP and National Research Council (CNPq) grants to H.F.C. and to C.L.C. (FAPESP Grant Nos. 08/57906-3 and 09/54164-9) are acknowledged. INFABIC is cofounded by CNPq and FAPESP.

REFERENCES

(1) Sun, Q.; Wang, Y. A.; Li, L. S.; Wang, D.; Zhu, T.; Xu, J.; Yang, C.; Li, Y. Bright, Multicoloured Light-emitting Diodes Based on Quantum Dots. *Nat. Photonics* **2007**, *1*, 717−722.

(2) Coleman, J. J.; Young, J. D.; Garg, A. Semiconductor Quantum Dot Lasers: A Tutorial. *J. Lightwave Technol.* **2011**, *29*, 499−510.

(3) Ip, A. H.; Thon, S. M.; Hoogland, S.; Voznyy, O.; Zhitomirsky, D.; Debnath, R.; Levina, L.; Rollny, L. R.; Carey, G. H.; Fischer, A. Hybrid Passivated Colloidal Quantum Dot Solids. *Nat. Nanotechnol.* **2012**, *7*, 577−582.

(4) Schaller, R. D.; Klimov, V. I. High Efficiency Carrier Multiplication in PbSe Nanocrystals: Implications for Solar Energy Conversion. *Phys. Rev. Lett.* **2004**, *92*, 186601-1−186601-4.

(5) Konstantatos, G.; Sargent, E. H. Solution-Processed Quantum Dot Photodetectors. *Proc. IEEE* **2009**, *97*, 1666−1683.

(6) Padilha, L. A.; Neves, A. A. R.; Rodriguez, E.; Cesar, C. L.; Barbosa, L. C.; Cruz, C. H. B. Ultrafast Optical Switching with CdTe Nanocrystals in a Glass Matrix. *Appl. Phys. Lett.* **2005**, *86*, 161111-1−161111-3.

DOI: 10.1021/jp512214p
J. Phys. Chem. B 2015, 119, 4294−4299

(7) Michalet, X.; Pinaud, F. F.; Bentolila, L. A.; Tsay, J. M.; Doose, S.; Li, J. J.; Sundaresan, G.; Wu, A. M.; Gambhir, S. S.; Weiss, S. Quantum Dots for Live Cells, in Vivo Imaging, and Diagnostics. *Science* **2005**, *307*, 538−544.
(8) Walling, M.; Novak, J.; Shepard, J. R. E. Quantum Dots for Live Cell and In Vivo Imaging. *Int. J. Mol. Sci.* **2009**, *10*, 441−491.
(9) Vieira, C. S.; Almeida, D. B.; de Thomaz, A. A.; Sadok Menna-Barreto, R. F.; dos Santos-Mallet, J. R.; Cesar, C. L.; Oliveira Gomes, S. A.; Feder, D. Studying Nanotoxic Effects of CdTe Quantum Dots in Trypanosoma Cruzi. *Mem. Inst. Oswaldo Cruz* **2011**, *106*, 158−165.
(10) Magde, D.; Webb, W. W.; Elson, E. Thermodynamic Fluctuations in a Reacting System - Measurement by Fluorescence Correlation Spectroscopy. *Phys. Rev. Lett.* **1972**, *29*, 705−708.
(11) Amos, W. B.; White, J. G. How the Confocal Laser Scanning Microscope entered Biological Research. *Biol. Cell* **2003**, *95*, 335−342.
(12) Rigler, R.; Mets, U.; Widengren, J.; Kask, P. Fluorescence Correlation Spectroscopy with High Count Rate and Low-background - Analysis of Translational Diffusion. *Eur. Biophys. J. Biophys.* **1993**, *22*, 169−175.
(13) Rigler, R.; Mets, U. Diffusion of Single Molecules Through a Gaussian Laser Beam. *Proc. SPIE - Laser Spectrosc. Biomol.* **1993**, *1921*, 239−248.
(14) Shimizu, K. T.; Neuhauser, R. G.; Leatherdale, C. A.; Empedocles, S. A.; Woo, W. K.; Bawendi, M. G. Blinking Statistics in Single Semiconductor Nanocrystal Quantum Dots. *Phys. Rev. B* **2001**, *63*, 205316-1−205316-5.
(15) Heuff, R. F.; Swift, J. L.; Cramb, D. T. Fluorescence Correlation Spectroscopy Using Quantum Dots: Advances, Challenges and Opportunities. *Phys. Chem. Chem. Phys.* **2007**, *9*, 1870−1880.
(16) Doose, S.; Tsay, J. M.; Pinaud, F.; Weiss, S. Comparison of Photophysical and Colloidal Properties of Biocompatible Semiconductor Nanocrystals Using Fluorescence Correlation Spectroscopy. *Anal. Chem.* **2005**, *77*, 2235−2242.
(17) Zhang, P. D.; Li, L. A.; Dong, C. Q.; Qian, H. F.; Ren, J. C. Sizes of Water-soluble Luminescent Quantum Dots Measured by Fluorescence Correlation Spectroscopy. *Anal. Chim. Acta* **2005**, *546*, 46−51.
(18) Schwille, P. Fluorescence Correlation Spectroscopy and its Potential for Intracellular Applications. *Cell Biochem. Biophys.* **2001**, *34*, 383−408.
(19) Krichevsky, O.; Bonnet, G. Fluorescence Correlation Spectroscopy: The Technique and its Applications. *Rep. Prog. Phys.* **2002**, *65*, 251−297.
(20) Hess, S. T.; Webb, W. W. Focal Volume Optics and Experimental Artifacts in Confocal Fluorescence Correlation Spectroscopy. *Biophys. J.* **2002**, *83*, 2300−2317.
(21) Schwille, P.; Haustein, E. Fluorescence Correlation Spectroscopy An Introduction to its Concepts and Applications Biophysics Textbook Online, http://www.biophysics.org/portals/1/pdfs/education/schwille.pdf.
(22) Zhang, H.; Wang, L. P.; Xiong, H. M.; Hu, L. H.; Yang, B.; Li, W. Hydrothermal Synthesis for High-quality CdTe Nanocrystals. *Adv. Mater.* **2003**, *15*, 1712.
(23) Zhang, H.; Zhou, Z.; Yang, B.; Gao, M. Y. The Influence of Carboxyl Groups on the Photoluminescence of Mercaptocarboxylic Acid-stabilized CdTe Nanoparticles. *J. Phys. Chem. B* **2003**, *107*, 8−13.
(24) Culbertson, C. T.; Jacobson, S. C.; Michael Ramsey, J. Diffusion Coefficient Measurements in Microfluidic Devices. *Talanta* **2002**, *56*, 365−373.
(25) Korson, L.; Drost-Hansen, W.; Millero, F. J. Viscosity of Water at Various Temperatures. *J. Phys. Chem.* **1969**, *73*, 34−39.
(26) Liedl, T.; Keller, S.; Simmel, F. C.; Radler, J. O.; Parak, W. J. Fluorescent Nanocrystals as Colloidal Probes in Complex Fluids Measured by Fluorescence Correlation Spectroscopy. *Small* **2005**, *1*, 997−1003.

DOI: 10.1021/jp512214p
J. Phys. Chem. B 2015, 119, 4294−4299